1521-009X/51/3/285–292$35.00
DRUG METABOLISM AND DISPOSITION

dx.doi.org/10.1124/dmd.122.001155
Drug Metab Dispos 51:285–292, March 2023

Quantification of Accurate Composition and Total Abundance of Homologous Proteins by Conserved-Plus-Surrogate Peptide Approach: Quantification of UDP Glucuronosyltransferases in Human Tissues[S]

Deepak Ahire, Mitesh Patel, Sujal V. Deshmukh, and Bhagwat Prasad

Department of Pharmaceutical Sciences, Washington State University (WSU), Spokane, Washington (D.A., B.P.) and Novartis Institutes for BioMedical Research, Cambridge, Massachusetts (M.P., S.V.D.)

Received October 7, 2022; accepted November 8, 2022

ABSTRACT

Characterization of accurate compositions and total abundance of homologous drug-metabolizing enzymes, such as UDP glucuronosyltransferases (UGTs), is important for predicting the fractional contribution of individual isoforms involved in the metabolism of a drug for applications in physiologically based pharmacokinetic (PBPK) modeling. Conventional targeted proteomics utilizes surrogate peptides, which often results in high technical and interlaboratory variability due to peptide-specific digestion leading to data inconsistencies. To address this problem, we developed a novel conserved-plus-surrogate peptide (CPSP) approach for determining the accurate compositions and total or cumulative abundance of homologous UGTs in commercially available pooled human liver microsomes (HLM), human intestinal microsomes (HIM), human kidney microsomes (HKM), and human liver S9 (HLS9) fraction. The relative percent composition of UGT1A and UGT2B isoforms in the human liver was 35:5:36:11:13 for UGT1A1:1A3:1A4:1A6:1A9 and 20:32:22:21:5 for UGT2B4:2B7:2B10:2B15:2B17. The human kidney and intestine also showed unique compositions of UGT1As and UGT2Bs. The reproducibility of the approach was validated by assessing correlations of UGT compositions between HLM and HLS9 (R^2> 0.91). The analysis of the conserved peptides also provided the abundance for individual UGT isoforms included in this investigation as well as the total abundance (pmol/mg protein) of UGT1As and UGT2Bs across tissues, i.e., 268 and 342 (HLM), 21 and 92 (HIM), and 138 and 99 (HKM), respectively. The CPSP approach could be used for applications in the in-vitro-to-in-vivo extrapolation of drug metabolism and PBPK modeling.

SIGNIFICANCE STATEMENT

We quantified the absolute compositions and total abundance of UDP glucuronosyltransferases (UGTs) in pooled human liver, intestine, and kidney microsomes using a novel conserved-plus-surrogate peptide (CPSP) approach. The CPSP approach addresses the surrogate peptide–specific variability in the determination of the absolute composition of UGTs. The data presented in this manuscript are applicable for the estimation of the fraction metabolized by individual UGTs towards better in vitro-to-in vivo extrapolation of UGT-mediated drug metabolism.

Introduction

Selective quantification of drug-metabolizing enzymes and transporter proteins (DMETs) using liquid chromatography–tandem mass spectrometry (LC-MS/MS)-based quantitative proteomics has significant utility in mechanistic and translational studies during drug discovery and development (Prasad et al., 2019). In particular, the DMET abundance data along with scaling factors such as microsomal protein per gram liver are used for the in-vitro-to-in-vivo extrapolation (IVIVE) of drug disposition. These data are also the foundation for the development of physiologically based pharmacokinetic (PBPK) modeling tools (Sharma et al., 2020; Ahmed et al., 2022). Proteomics data on the effect of age (Prasad et al., 2013; Ahire et al., 2022a), disease conditions (Wang et al., 2016; Drozdzik et al., 2020; Vildhede et al., 2020; El-Khateeb et al., 2021), differential tissue expression (Basit et al., 2020; Wenzel et al., 2021), and interspecies differences (Liao et al., 2018; Basit et al., 2022) on DMETs have been used in PBPK modeling. However, interlaboratory technical variability in DMET abundance data (Wegler et al., 2017) poses a significant challenge in utilizing the reported values. Furthermore, the metabolism or transport of a drug often involves more than one enzyme or transporter. DMET proteins are generaly homologous and share a broad substrate selectivity. For instance, the protein sequence similarities of UDP glucuronosyltransferase (UGT) 1As and 2Bs share 67%–95% and 77%–95% amino acid sequences, respectively (Meech et al., 2019), and multiple UGTs are often involved in the glucuronidation of a drug. In recent years, the use of recombinant UGTs has emerged as a useful in vitro approach for identifying isoforms involved in glucuronidation. However, the accurate estimation of their fractional contribution (f_m) or extrapolation of drug clearance requires that the data generated using recombinant UGTs are normalized by the

BP is the cofounder of Precision Quantomics Inc and recipient of research funding from Bristol Myers Squibb, Genentech, Gilead, Merck, Novartis, Takeda, and Generation Bio.

dx.doi.org/10.1124/dmd.122.001155.

[S]This article has supplemental material available at dmd.aspetjournals.org.

ABBREVIATIONS: ABC, ammonium bicarbonate; CPSP, conserved-plus-surrogate peptide; DMET, drug-metabolizing enzyme and transporter protein; HIM, human intestinal microsomes; HKM, human kidney microsomes; HLM, human liver microsomes; IVIVE, in-vitro-to-in-vivo extrapolation; LC-MS/MS, liquid chromatography–tandem mass spectrometry; PBPK, physiologically based pharmacokinetic; REF, relative expression factor; rUGT, recombinant UGT system; SIL, stable isotope–labeled; UGT, UDP glucuronosyltransferase.

tissue abundance of individual UGTs (Rowland et al., 2008). Therefore, accurate characterization of the relative and absolute composition of UGTs is critical for IVIVE of UGT-mediated metabolism.

The conventional targeted proteomics approach that relies on a surrogate peptide(s) as a calibrator is routinely used for quantifying DMETs (Prasad et al., 2019). However, the large interlaboratory variability has limited the application of reported DMET abundance data in accurately predicting in vivo glucuronidation (Wegler et al., 2017). Although the total proteomics approach using untargeted proteomics data has the potential to address this challenge, this approach is mainly applicable to highly abundant proteins and, hence, offers limited applications in the quantification of low abundant transmembrane DMET proteins (Wiśniewski, 2017).

The relative expression factor (REF) approach (eq. 1) has been used for IVIVE of drug metabolism (Parvez et al., 2021) and transport (Harwood et al., 2016; Kumar et al., 2020) data from recombinant systems to human tissues. In general, relative quantification is sufficient for estimating REF values by quantifying a target protein in a recombinant system versus human tissues as long as the data are generated in a single laboratory using an optimized surrogate peptide and digestion protocol. If REF values are based on DMET quantification in different laboratories, they will likely be confounded by technical variability in protein abundance measurement. The interlaboratory variability in quantitative proteomics is mainly caused by differences in surrogate peptide–specific characteristics such as solubility, stability, and calibrator quality as well as digestion efficiency (Ahire et al., 2022b). Moreover, interday variability in digestion efficiency is also commonly observed (Wegler et al., 2017). In addition, the lack of appropriate use of internal/external standards during sample preparation and the use of different peptides could also lead to technical variabilities.

$$REF = \frac{protein\ abundance\ in\ tisue}{protein\ abundance\ in\ the\ recombinant\ system} \quad (1)$$

To address the above-mentioned issues, we developed a novel approach comprised of universal conserved-plus-surrogate peptide (CPSP) to determine the accurate compositions (relative distributions) of homologous DMETs and applied it to measure UGT1A and UGT2B pies in human liver microsomes (HLM), human intestinal microsomes (HIM), and human kidney microsomes (HKM). First, we identified peptides that were conserved in multiple isoforms of UGT1As and UGT2Bs. Then, the conserved peptides of UGT1s and UGT2Bs were used as calibrators for quantifying UGT protein abundance in the recombinant UGT systems (rUGT) samples (Fig. 1). Finally, the standardized rUGTs were used as calibrators that relied on individual surrogate peptide signals (Fig. 1) to determine UGT levels in the pooled HLM, HIM, and HKM. These data were then used to quantify the percentage of abundance of individual UGT1As and UGT2Bs in each tissue. The HLM data were compared with UGT pies obtained in HLS9 fractions. The analysis of conserved peptides also provided the total or cumulative abundance of UGT1As and UGT2Bs in each tissue. The proposed universal approach is less prone to peptide-specific characteristics as it utilizes a single conserved peptide to determine absolute levels in the recombinant systems. The use of recombinant proteins in the second step addresses the limitation of interday or interlaboratory variability in trypsin digestion. Since this approach only requires conserved peptide standards, it is also a cost-effective method.

Materials and Methods

Materials. The custom-synthesized stable isotope–labeled (SIL) surrogate peptides for 13 UGT isoforms were purchased from Thermo Fisher Scientific (Rockford, IL) (Supplemental Table 1). The purified calibrator conserved peptide (IPQTVLWR and VLWR; purity >95%) with accurate concentrations determined by the amino acid analysis were purchased from Vivitide (Gardner, MA). Chloroform, methanol, mass spectrometry–grade acetonitrile, and formic acid were purchased from Fisher Scientific (Fair Lawn, NJ). The protein quantification bicinchoninic acid kit was procured from Pierce Biotechnology (Rockford, IL). Ammonium bicarbonate (ABC) (98% pure), dithiothreitol, iodoacetamide, and trypsin were purchased from Thermo Fisher Scientific. Human serum albumin and bovine serum albumin were obtained from Calbiochem (Billerica, MA) and Thermo Fisher Scientific, respectively.

Procurement of Pooled Human Tissue Subcellular Fractions and Recombinant UGTs. Pooled HLM (150 donors) was obtained from BioIVT Inc.

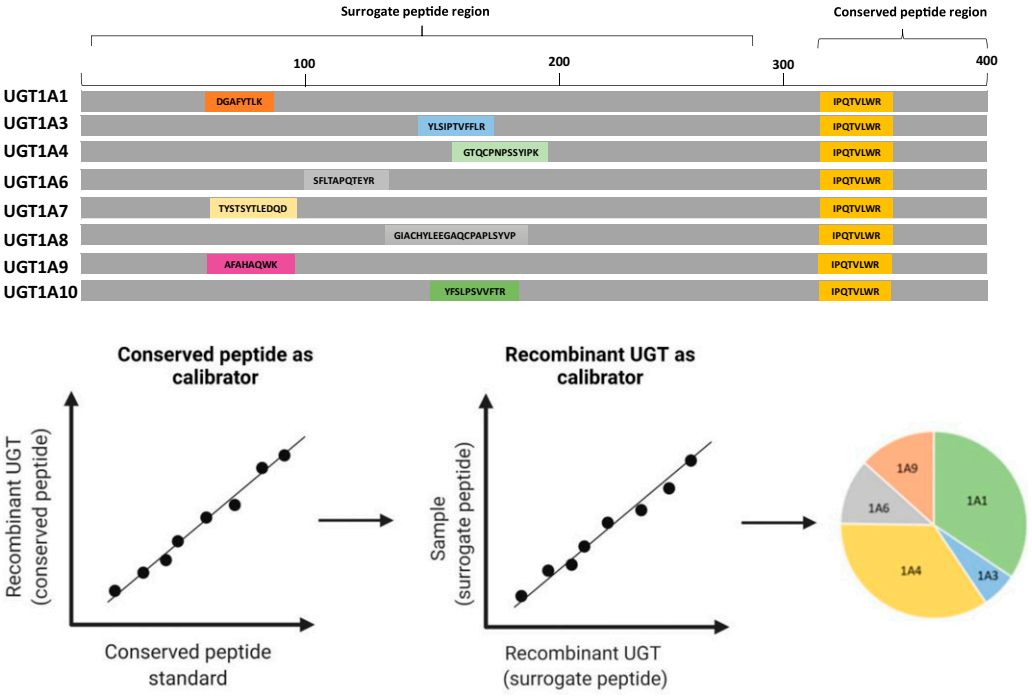

Fig. 1. CPSP approach.

TABLE 1

Comparison of the conventional surrogate peptide and CPSP approaches

Attribute	Surrogate Peptide Approach	CPSP Approach
Calibration method	One-step calibration (surrogate peptide as a calibrator)	Two-step calibration (conserved peptide as a calibrator for recombinant proteins and recombinant proteins as a calibrator for tissue samples)
Trypsin digestion variability	Peptide-specific digestion variability	Not applicable. A single peptide is used
Potential for interlaboratory variability	High	Low
Application	Relative protein abundance across samples	Relative protein abundance across proteins and samples. Relative distribution (absolute pies). Total abundance of homologous proteins.
Cost	Expensive as it requires peptide standards for each protein	Economical as it requires only a single conserved peptide standard

(Westbury, NY), whereas pooled HKM (8 donors), and pooled HIM (15 donors) were procured from Xenotech (Kansas City, KS). Pooled HLS9 (50 donors) and 13 recombinant UGT preparations (UGT1A1, 1A3, 1A4, 1A6, 1A7, 1A8, 1A9, 1A10, 2B4, 2B7, 2B15, 2B10, and 2B17) were procured from Corning Life Sciences (Corning, NY).

Conserved and Surrogate Peptide Selection. The surrogate peptide selection approach is well established (Kamiie et al., 2008), whereas the criteria for conserved peptide selection used in the CPSP approach was developed in this study (Fig. 1). Briefly, an ideal conserved peptide should be present in all target homologous proteins, be retainable in reversed-phase liquid chromatography column, contain more than three amino acids, be ionizable in mass spectrometer source, and be formed after trypsin digestion. Moreover, we confirmed by homology search that the conserved peptide (Table 1) is only present in the target homologous proteins (e.g., UGT1A and UGT2B isoforms). Using these criteria, IPQTVLWR and VLWR were selected as the target conserved peptides for the quantification of UGT1As and UGT2Bs in rUGTs, respectively (Fig. 2; Supplemental Table 1). In the next step, using rUGTs as a calibrator, individual UGT proteins in tissue samples were quantified using a minimum of two surrogate peptides except for UGT1A3, UGT1A9, UGT1A10 (Supplemental Table 1). The approach was further applied to identify conserved peptides for other clinically relevant DMETs (Table 2).

Protein Digestion by Trypsin. The recombinant UGTs and pooled HLM, HIM, HKM, and HLS9 (1 mg/ml protein concentration) were mixed with ABC buffer (100 mM, pH 7.8), dithiothreitol (250 mM), and bovine serum albumin (0.02 mg/mL) and incubated at 95°C for 10 minutes (protein denaturation and reduction step). Followed by cooling at room temperature for 10 minutes, the protein mixture was alkylated by iodoacetamide (500 mM) in the dark for 30 minutes. The alkylated sample was subjected to protein precipitation by adding ice-cold acetone and incubated at −80°C (in a deep freezer) for 1 hour. The precipitated protein sample was centrifuged at 16,000*g* for 10 minutes. The resultant pellet was washed with 500 mL ice-cold methanol and dried under vacuum for 30 minutes. The dried protein pellet was resuspended in ABC buffer (50 mM, pH 7.8) and digested by trypsin (20 μL; protein/trypsin ratio ∼80:1) at 37°C for 16 hours with gentle shaking (300 rpm). The digestion was stopped by adding 5 μL of 0.5% formic acid, and the sample was centrifuged at 8000*g* for 10 minutes (4°C). Five microliters of the internal standard mix (i.e., a cocktail of SIL peptides; Supplemental Table 1) was added to 45 μL of the digested sample, vortex mixed, and transferred to a liquid chromatography–mass spectrometry vial.

LC-MS/MS Analysis of the Conserved and Surrogate Peptides in Recombinant Systems and Tissue Fractions. The conserved and surrogate peptides (Supplemental Table 1) were analyzed using an M-class microflow Waters UPLC system coupled with Waters Xevo TQ-XS LC-MS/MS instrument. The peptides were separated on the Acquity UPLC HSS T3 column (Waters, Milford, MA). The optimized LC-MS/MS acquisition parameters, including the liquid chromatography gradient program, are provided in Supplemental Table 2. The LC-MS/MS data were analyzed using Skyline 20.1 (University of Washington, Seattle, WA), where peptide peaks were identified by matching the retention time with the SIL peptide and alignment of the selected precursor ion to the respective product ion fragments. A previously optimized data analysis approach (Ahire et al., 2021) that considers the internal standard protein (bovine serum albumin) and the SIL peptide was used. The experiments were performed in triplicates, and the CV was measured.

In the first step of UGT quantification, we employed an internal calibration (spiked-in) method where the standardized SIL-conserved peptides, IPQTVLWR and VLWR, were used as calibrators to measure the levels of individual UGT1As and UGT2Bs in the recombinant UGT systems, i.e., UGT1A1, 1A3, 1A4, 1A6, 1A7, 1A8, 1A9, and 1A10 and UGT2B4, 2B7, 2B10, 2B15, and 2B17. The purity of the conserved peptides was assessed by amino acid analysis or back calculation from unlabeled peptides as discussed in the Supplemental file. In the second step, we used the surrogate peptide response of individual UGTs in the calibrated recombinant UGTs to quantify UGT levels in the tissue fractions using an external calibration method as illustrated in Fig. 1. In addition, the total UGT1As and UGT2Bs were quantified in biologic samples based on the respective conserved peptide responses.

Data Analysis and Validation. The UGT abundance in human tissues was compared with the literature-reported meta-analysis values compiled within Simcyp software (Certara, NJ). The total abundance of UGT1A and UGT2B calculated using conserved peptide was compared using Student's *t* test with the sum of all UGT1As and UGT2Bs. The correlation between UGT abundances in HLM versus HLS9 was tested using Pearson regression analysis.

Results

Selection of Conserved Peptides for Clinically Relevant DMETs. A list of selected conserved tryptic and chymotryptic peptides is provided in Table 2 for quantification of clinically relevant cytochrome P450s, UGTs, sulfotransferases, glutathione S-transferases, flavin-containing monooxygenases, aldehyde dehydrogenases, alcohol dehydrogenases, carboxylesterases, organic anion transporting polypeptides, and organic anion and organic cation transporters. These peptides can be used for the quantification of accurate composition and the total or cumulative abundance of respective homologous proteins in complex biologic samples such as HLM, HIM, HKM, and HLS9 samples using the optimized CPSP approach discussed here.

Quantification of UGT Isoforms in the Recombinant System Using Conserved Peptides as Calibrators. The two stable-labeled calibrator peptides (IPQTVLWR and VLWR) were separated on a liquid chromatography column with a retention time of 14.7 and 13.0, respectively (Supplemental Fig. 1). The calibration curves of the conserved

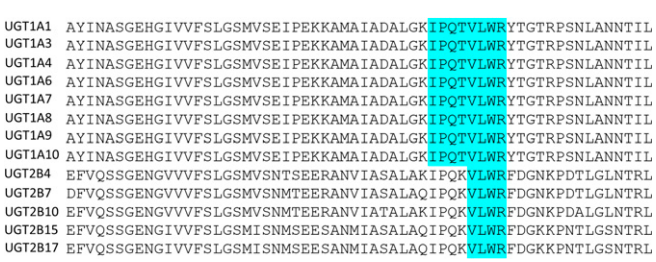

Fig. 2. Conserved peptide sequences of UGT1As and UGT2Bs.

TABLE 2

Predicted conserved peptide sequences of DMET proteins after trypsin or chymotrypsin digestion

Homologous Proteins	Tryptic Peptides	Chymotryptic Peptides
P450s		
CYP1A1 and CYP1A2	NPHLALSR, QALVR, and QGDDFK	GKNPHL, DTIRQAL, VRQGDDF, and DTVTTAISW
CYP2A6, CYP2C8, and CYP2C9	FDYK	
CYP2B6 and CYP2E1		AGTETTSTTL
CYP2C8 and CYP2C9	FDYK, FSLTTLR, SIEDR, HPEVTAK, NYLIPK, and FSLTTLR	EAVKEAL and RKTKASPCDPTF
CYP2C8 and CYP2E1	FSLTTLR	
CYP3A4, CYP3A5, and CYP3A7	ECYSVFTNR, SLLSPTFTSGK, and ETQIPLK	NNPQDPF and VENTKKL
CYP3A4 and CYP3A5,	ECYSVFTNR, SLLSPTFTSGK, ETESHK, and VLQNFSFKPCK	GVNIDSL, ATHPDVQQKL, and KPCKETQIPL
CYP3A4 and CYP3A7	ECYSVFTNR, SLLSPTFTSGK, EAETGKPVTLK, YWTEPEK, and VLQNFSFKPCK	GIPGPTPLPF, RREAETGKPVTL, GVNIDSL, VENTKKL, and SKKNKDNIDPY
UGTs		
UGT1A1, UGT1A3, UGT1A4, UGT1A6, UGT1A7, UGT1A8, UGT1A9, and UGT1A10	IPQTVLWR	INASGEHGIVVF, GKIPQTVL, TGTRPSNL, LPQNDL, ITHAGSHGVY, KAVINDKSY, HKDRPVEPL, RPAAHDL, and GKKGRVKKAHKSKTH
UGT2B4, UGT2B7, and UGT2B10		VQSSGENGVVVF, IPQNDL, GHPKTRAF, and ITHGGANGIY
UGT2B4 and UGT2B10		AKIPQKVL and SRIHHDQPVKPL
UGT2B4 and UGT2B7		DGNKPDTL and RVAAHDL
UGT2B4 and UGT2B15		ACVATVIF
UGT2B7 and UGT2B10		ASSASIL
UGT2B4, UGTB7, UGT2B10, UGT2B15, and UGT2B17	VLWR	
GSTs		
GSTA1, GSTA2, GSTA3, and GSTA5		VQTRAIL, GKDIKERAL, VGNKL, and KTRISNLPTVKKF
GSTA1 and GSTA2	SAEDLDK, AILNYIASK, YFPAFEK, SHGQDYLVGNK, ISNLPTVK, FLQPGSPR, LVQTR, YNLYGK, YFPAFEK, and ISNLPTVK	IKSAEDL, IEGIADL, KSHGQDY, and SRADIHL
GSTA1, GSTA3, and GSTA5		ISSFPL, EEARKIF, and RNDGSL
GSTA3 and GSTA5	AILNYIASK, YFPAFEK, ISNLPTVK, FLQPGSPR, LVQTR, YNLYGK, YFPAFEK, and ISNLPTVK	
GSTA4 and GSTA5	LVQTR	
GSTM1, GSTM2, GSTM3, and GSTM4		DRSQW and DFPNLPY
GSTM1, GSTM2, and GSTM5		IARKHNL and DAFPNL
GSTM1 and GSTM4	ITQSNAILCYIAR and HNLCGETEEEK	IDGAHKITQSNAIL and CGETEEEKIRVDIL
GSTM2 and GSTM4	SQWLNEK and ITQSNAILR	
GSTM3 and GSTM4	ITQSNAILR	
SULTs		
SULT1A1, SULT1A2, SULT1A3, and SULT1A4	VVYVAR, ILEFVGR, and TTFTVAQNER	QARPDDL, DQKVKVVY, QHVQEW, SRTHPVL, TVAQNERF, VSQIL, and QHVQEW
SULT1A1 and SULT1A2	VPFLEFK	ISTYPKSGTTW, EKCHRAPIF, and VARNAKDVAVSY
SULT1A1, SULT1A3, and SULT1A4	FDADYAEK	
SULT1A3 and SULT1A4	DTPPPR, DVAVSYYHFHR, and AHPEPGTWDSFLEK	INTYPKSGTTW and VARNPKDVAVSY
SULT2A1 and SULT2B1		SSKAKVIY
FMOs		
FMO1, FMO2, and FMO5	GQYFHSR	
FMO1, FMO2, and FMO3		EPTCF
FMO1 and FMO2		HSRQY and IFPAHL
FMO1 and FMO3		GPCSPY
FMO2 and FMO3		TETSAIF
FMO3 and FMO5	ASIYK	HSRDY and TDPKL
ALDHs		
ALDH1A1, ALDH1A2, and ALDH1A3	VTLELGGK	TGSTEVGKL
ALDH1A1 and ALDH1A2		TRHEPIGVCGQIIPW
ALDH1A1 and ALDH1A3		IESGKKEGAKL
ALDH1A2 and ALDH1A3		IAFTGSTEVGK
ADHs		
ADH1A, ADH1B, and ADH1c	NPESNYCLK, IDAASPLEK, AAGAAR, IIAVDINK, ELGATECINPQDYK, and KPIQEVLK	GATECINPQDY, KKPIQEVL, and EKINEGF
ADH1A and ADH1B		ITHVLPF
OATPs		
OATP1B1, OATP1B3, and OATP2B1		IDDF and VGAW
OATP1B1 and OATP1B3	LHRPK, NYSAHLGECPR, and IVQPELK	RGIGETPIVPL, AKEGHSSL, SIISSIPF, EPVCGNNGITY, and QNRNY
OATP1B3 and OATP2B1		GISY
OCTs		
OCT1 and OCT3		SPAEEL, ALPHW, and VNAEL

TABLE 2 *continued*

Homologous Proteins	Tryptic Peptides	Chymotryptic Peptides
CESs		
CES1 and CES2		AKPPL

ADH, alcohol dehydrogenase; ALDH, aldehyde dehydrogenase; CES, carboxylesterase; FMO, flavin-containing monooxygenase; GST, glutathione S-transferase; OAT, organic anion transporter; OATP, organic anion transporting polypeptide; OCT, organic cation transporters; P450, cytochrome P450; SULT, sulfotransferase.

peptides were linear across 29–925 fmol/μL and 2.67–170.75 fmol/μL, respectively with $R^2 > 0.98$ (Supplemental Fig. 2). Based on the signal-to-noise ratio criteria of 5:1, the lower limit of quantification was estimated to be 0.36 and 0.65 fmol/μL for IPQTVLWR and VLWR, respectively. The total abundance of UGT1As and UGT2Bs in human liver microsomes was 268.0 and 341.7 pmol/mg protein (Fig. 3). The abundance (pmol/mg protein) of various UGT1As in commercially available recombinant systems was within a 3.7-fold range (Table 3), where the abundances of UGT1A1 and UGT1A3 were comparably followed by UGT1A8 > UGT1A10 > UGT1A6 > UGT1A9 > UGT1A4, and > UGT1A7. Similarly, a 9.9-fold range was noted in the abundances of recombinant UGT2Bs with the following ranking of UGT2B15 > UGT2B17 > UGT2B7 > UGT2B4, and > UGT2B10.

Quantification of UGT1A and UGT2B Isoforms in HLM, HLS9, HIM, and HKM Using rUGTs as Calibrators. The liver protein abundance (pmol/mg protein) values of UGT1As and UGT2Bs are shown in Table 3. In general, the abundance of individual UGTs was higher in the recombinant systems, followed by HLM except for UGT1A6, UGT1A9, and UGT2B17, which were higher in HKM and HIM, respectively. The accurate composition of UGT1As showed almost an equal abundance of UGT1A1 and UGT1A4 in HLM, followed by UGT1A9 > UGT1A6, and > UGT1A3. Whereas among UGT2Bs, UGT2B7 showed a higher abundance in HLM followed by UGT2B10, UGT2B15, and UGT2B4, UGT2B17 accounted for less than 5% of total UGT abundance in HLM UGT2Bs pies (Fig. 4). As expected, the HLS9 followed similar trends (Fig. 5; $R^2 > 0.91$) in the expression of UGT1As and UGT2Bs (Supplemental Fig. 3). The average UGT abundance in the HLS9 was approximately sixfold lower compared with HLM. UGT1A1, UGT1A3, UGT1A10, UGT2B7, and UGT2B17 are expressed in the human intestine, and UGT1A6, UGT1A9, and UGT2B7 are expressed in the human kidney (Basit et al., 2020). UGT1A1, UGT1A3, UGT2B7, and UGT2B17 are the common UGTs expressed in both the human liver and intestine (Basit et al., 2020). The abundance of UGT1A1, UGT1A3, and UGT2B7 is ∼9-, 13-, and 7-fold lower in HIM than in HLM (Fig. 4; Supplemental Table 3), whereas the abundance of UGT2B17 is approximately threefold higher in HIM as compared with HLM (Fig. 4). The abundance of UGT1A6 and UGT1A9 is ∼1.8- and 2.2-fold higher in HKM than in HLM, respectively; however, UGT2B7 abundance was 1.8-fold lower in HKM than HLM (Fig. 4; Supplemental Table 3).

Using the CPSP approach, we confirmed that UGT1A1 is the most abundant UGT1A isoform in HIM, followed by UGT1A10 and UGT1A3, whereas, amongst UGT2Bs, the abundance of UGT2B17 was approximately threefold higher than UGT2B7 in HIM (Fig. 4). Only UGT1A6, UGT1A9, and UGT2B7 are expressed in HKM. The estimated UGT abundances in HLM using the CPSP approach were similar (within twofold) to the metanalysis values reported by Simcyp (Certara, NJ) except for UGT2B17 and UGT2B10 (Table 3).

UGT2B17 abundance was around threefold higher, whereas UGT2B10 abundance was tenfold higher in our study compared with the metanalysis values. This discrepancy is likely because both UGT2B17 and UGT2B10 are highly polymorphic with ethnic variability in their gene deletion (Xue et al., 2008) or splicing polymorphism (Fowler et al., 2015; Sipe et al., 2020), respectively. UGT1A7 and UGT1A8 were only detected in the recombinant system but not in HLM, HIM, HKM, or HLS9 fractions. UGT1A7 and UGT1A8 are highly homologous proteins, and their surrogate peptides, TYSTSYTLEDQD and GIACHYLEEGAQCPAPLSYVPR, show poor response in LC-MS/MS. Therefore, to further confirm our findings, we used a highly sensitive conserved peptide (YFSLPSVVFAR) for the cumulative quantification of UGT1A7, UGT1A8, and UGT1A9. Although YFSLPSVVFAR was detected in HLM, HLS9, and HKM because of UGT1A9 expression in these tissues, the same peptide was below the lower limit of quantification in HIM. Further, the total UGT1A abundance data also indicate that the expression of UGT1A7 and UGT1A8 is negligible in HIM as compared with the detected isoforms.

Discussion

Here, we developed a novel CPSP approach for the quantification of homologous proteins (e.g., UGTs). Although the conventional surrogate peptide–based approach is a routine method for the determination of UGT abundance, the data on UGT abundance from different laboratories are highly variable, which, in turn, leads to inaccurate estimation of the absolute composition of UGTs. In particular, protein digestion is likely associated with inconsistent and incomplete recovery of individual surrogate peptides. Ideally, the use of

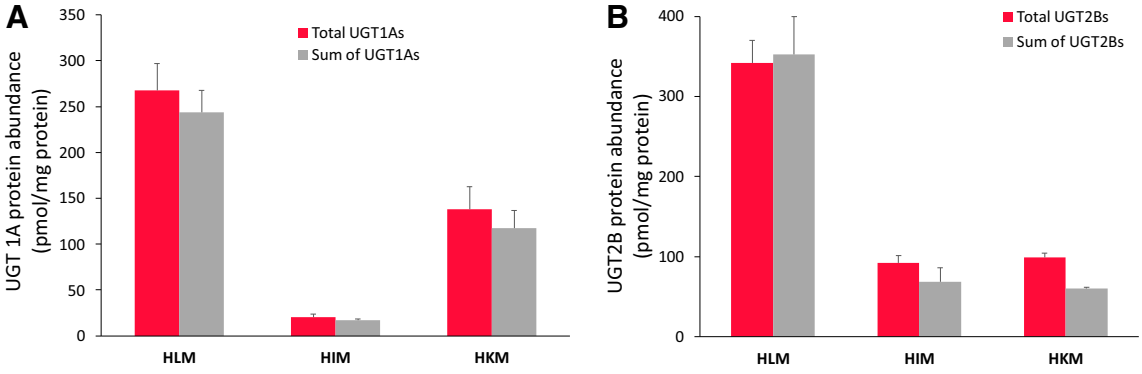

Fig. 3. Comparison of the total abundance and the sum of an individual abundance of UGT1As (A) and UGT2Bs (B) in HLM, HIM, and HKM.

TABLE 3

UGT abundance (pmol/mg microsomal protein) in the recombinant system and pooled HLM

UGT Isoform	Recombinant System	HLM	
		CPSP Data (Present Study)	Meta-Analysis (Reported)
UGT1A1	454.35 ± 49.69	85.01 ± 4.42	48 ± 11.52
UGT1A3	407.10 ± 54.24	12.57 ± 2.37	23 ± 8.28
UGT1A4	217.98 ± 10.43	88.26 ± 8.63	52 ± 13.52
UGT1A6	276.67 ± 17.07	26.92 ± 1.87	20 ± 6.00
UGT1A7	122.30 ± 16.38	<LLOQ	NR
UGT1A8	332.22 ± 24.31	<LLOQ	NR
UGT1A9	240.17 ± 35.79	31.14 ± 2.45	31 ± 9.30
UGT1A10	308.56 ± 31.82	<LLOQ	NR
UGT2B4	145.73 ± 19.26	71.09 ± 3.48	54 ± 15.12
UGT2B7	218.53 ± 24.33	112.83 ± 6.08	71 ± 21.58
UGT2B10	43.64 ± 3.29	76.46 ± 16.04	6.5 ± 1.95
UGT2B15	430.97 ± 12.65	75.05 ± 5.13	39 ± 13.26
UGT2B17	252.18 ± 19.77	16.80 ± 4.97	5.9 ± 1.65

LLOQ, lower limit of quantification; NR, not reported.

purified protein standards as calibrators can address the problem of inconsistent and incomplete trypsin digestion (Prasad et al., 2019). In the absence of purified UGT proteins, the two-step CPSP method used in this study addresses 1) inconsistency or peptide-specific variability in the first step by utilizing a single conserved peptide for the quantification of recombinant UGTs (single conserved peptide standard against different UGT isoforms) and 2) incomplete digestion in the second step by quantifying surrogate peptide responses in tissue fractions against the calibrated recombinant UGTs (recombinant protein standard against protein). Using the CPSP approach, we estimated the composition of UGT1As and UGT2Bs in human tissue fractions, which is important for estimating the fractional contribution of individual UGTs in drug glucuronidation. Although we only showed the application of the CPSP approach for UGT quantification, the conserved peptides listed in Table 2 could be used for determining the absolute composition or ratio of other homologous DMET proteins.

Although UGT abundance values are reported in previous studies (Izukawa et al., 2009; Harbourt et al., 2012; Fallon et al., 2013; Achour et al., 2014; Margaillan et al., 2015; Achour et al., 2017; Couto et al., 2020), the data provided in this manuscript is the first effort to estimate the absolute composition of these homologous enzymes. We estimated that in the intestine, UGT1A1 and UGT1A10 are comparable (within twofold), whereas UGT2B17 was threefold higher than UGT2B7. These data suggest that UGT2B17, UGT1A10, and UGT1A1 are important for the first-pass metabolism of drugs and natural products. These data are relevant in interpreting variability in

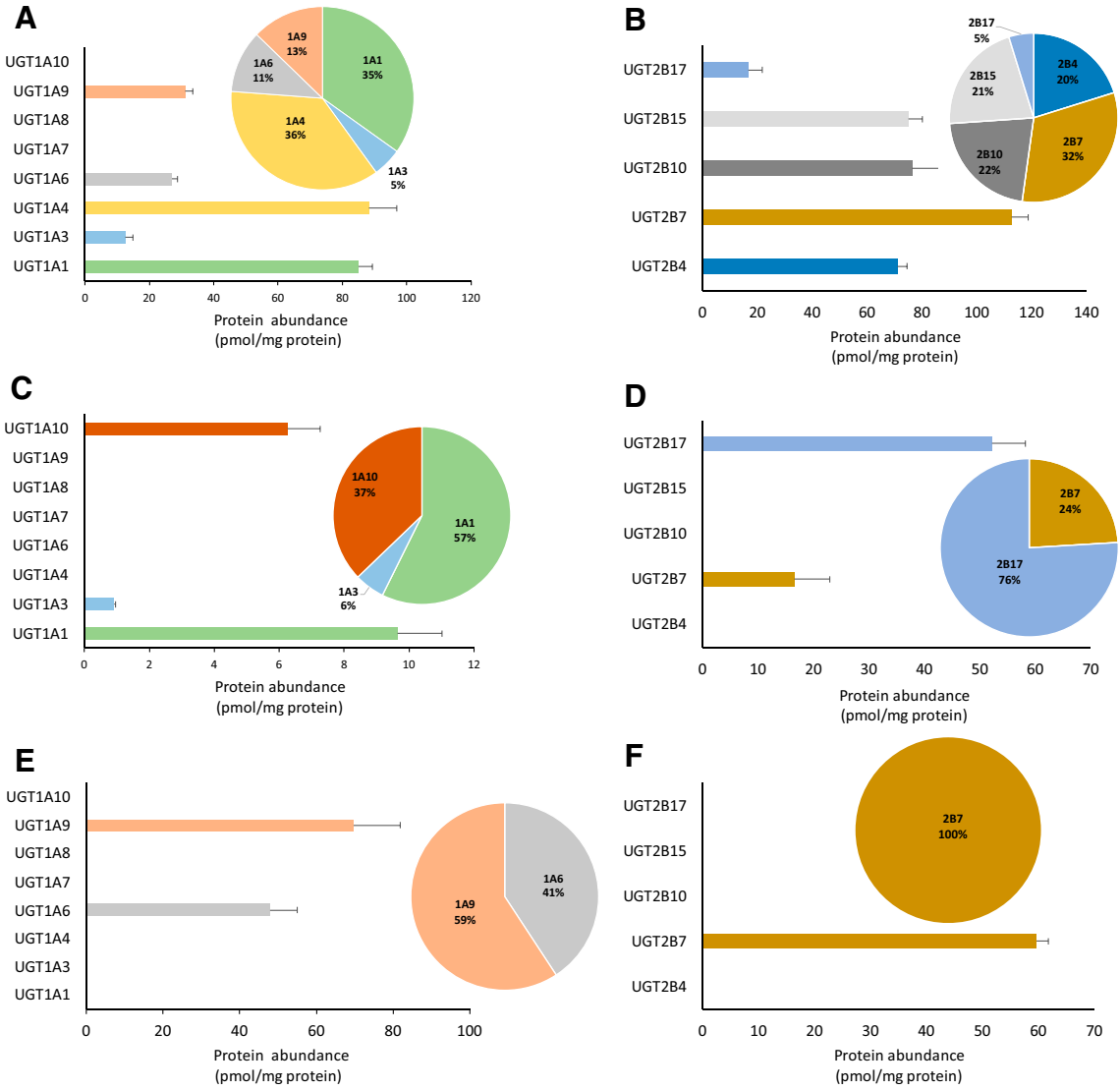

Fig. 4. Protein abundance of the major UGT1As and UGT2Bs using the CPSP approach in HLM (A and B), HIM (C and D), and HKM (E and F). Inset shows the fractional abundance of individual UGT1As and UGT2Bs in the microsomal fractions.

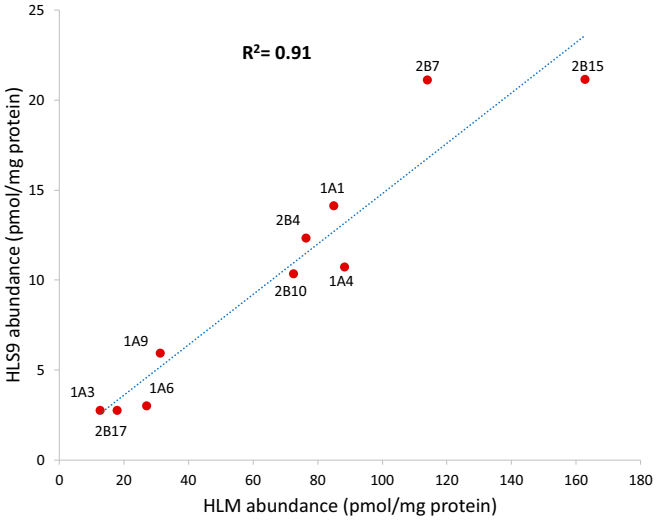

Fig. 5. Correlation of UGT abundance values between HLM and HLS9.

UGT1A1 and UGT2B17 that are highly polymorphic with promoter region single nucleotide polymorphisms (Iyer et al., 2002; Liu et al., 2007) and gene deletion (Xue et al., 2008; Wang et al., 2012; Bhatt et al., 2018), respectively. A high abundance of UGT1A9, UGT2B7, and UGT1A6 in the kidney should also be considered in the PBPK modeling of substrates of these enzymes, such as furosemide, morphine, zidovudine, acetaminophen, and aspirin.

Protein quantification using a surrogate peptide approach relies on the trypsin digestion efficiency of a protein. However, the trypsin digestion efficiency can be highly variable due to peptide-specific factors such as the trypsin/protein ratio, incubation time, temperature, pH, surfactant concentration, steric hindrance of amino acids, and stability of trypsin (Bhatt and Prasad, 2018). In addition, the vendor-to-vendor variability in the surrogate peptide quality, stability, and solubility brings added interlaboratory variability in the quantification of protein abundance using the surrogate peptide approach. These variables lead to differences in the accurate UGT compositions of DMET proteins and add ambiguity to the reported abundance values. The CPSP approach addresses the above-mentioned limitations of surrogate peptide–based quantification of DMET proteins. The major advantage of the CPSP approach is that it addresses the issue of inconsistent trypsin digestion across different surrogate peptides, which is considered to be the major factor leading to high interlaboratory variabilities in targeted proteomics (Prasad et al., 2019). The CPSP approach is also a cost-effective method for the targeted quantification of proteins as it does not require the procurement of multiple synthetic surrogate peptides. Finally, this approach provides quantification of the total or cumulative abundance of multiple homologous proteins, which can be used for predicting the overall drug-metabolizing or transport capacity of an individual organ.

The rate of glucuronide formation determined using commercially available recombinant systems is generally expressed in the units of pmol/min per mg of protein. Since UGT abundance per mg protein is not available in these systems, it is required that UGT quantification is performed to normalize the activity data to the amount of enzyme. The metabolic clearance from the recombinant enzyme system to a particular tissue can be extrapolated with an assumption that the recombinant proteins are fully active and that the Michaelis-Menten constant (K_m) remains similar between the recombinant system and the tissue. Also, the commercial vendors of recombinant proteins could use this approach for normalizing UGT abundance in their products. However, the recombinant UGTs could be either misfolded or have some structural differences from native enzymes present in the tissue sample (Gasser et al., 2008), which produce less active protein as compared with the native UGTs. Nevertheless, the UGT abundance data are useful in IVIVE as long as the difference in the protein abundance-normalized UGT activity (per pmol protein) between recombinant enzyme and tissue fraction remains substrate independent.

The trypsin digestion efficiency for conserved peptide formation may not be 100% in the recombinant or tissue fraction samples. However, this approach is better than using peptide standards as a calibrator. Considering that our data corroborates with the meta-analysis data (Table 3) except for the abundance of highly polymorphic UGTs (UGT2B10 and UGT2B17), we believe that the digestion efficiency is consistent between recombinant enzyme and tissue fraction.

In summary, the novel CPSP method described here could serve as a universal and cost-effective approach for the quantification of accurate compositions and total or cumulative abundance of UGT1As and UGT2Bs in human tissues. This approach addresses the trypsin digestion variability of the current surrogate peptide approach and reduces the peptide-specific variability due to solubility and stability issues. Furthermore, this approach eliminates the need to purchase multiple surrogate peptide standards for the quantification of DMET proteins. Finally, the conserved peptide quantification data can be provided by the commercial vendors of recombinant UGT proteins that can be used to normalize the UGT abundance between systems.

Authorship Contributions

Participated in research design: Ahire, Patel, Deshmukh, Prasad.
Conducted experiments: Ahire.
Performed data analysis: Ahire, Prasad.
Wrote or contributed to the writing of the manuscript: Ahire, Patel, Deshmukh, Prasad.

References

Achour B, Dantonio A, Niosi M, Novak JJ, Fallon JK, Barber J, Smith PC, Rostami-Hodjegan A, and Goosen TC (2017) Quantitative Characterization of Major Hepatic UDP-Glucuronosyltransferase Enzymes in Human Liver Microsomes: Comparison of Two Proteomic Methods and Correlation with Catalytic Activity. *Drug Metab Dispos* **45**:1102–1112.

Achour B, Russell MR, Barber J, and Rostami-Hodjegan A (2014) Simultaneous quantification of the abundance of several cytochrome P450 and uridine 5′-diphospho-glucuronosyltransferase enzymes in human liver microsomes using multiplexed targeted proteomics. *Drug Metab Dispos* **42**:500–510.

Ahire D, Basit A, Christopher LJ, Iyer R, Leeder JS, and Prasad B (2022a) Interindividual Variability and Differential Tissue Abundance of Mitochondrial Amidoxime Reducing Component Enzymes in Humans. *Drug Metab Dispos* **50**:191–196.

Ahire D, Kruger L, Sharma S, Mettu VS, Basit A, and Prasad B (2022b) Quantitative Proteomics in Translational Absorption, Distribution, Metabolism, and Excretion and Precision Medicine. *Pharmacol Rev* **74**:769–796.

Ahire DS, Basit A, Karasu M, and Prasad B (2021) Ultrasensitive Quantification of Drug-metabolizing Enzymes and Transporters in Small Sample Volume by Microflow LC-MS/MS. *J Pharm Sci* **110**: 2833–2840.

Ahmed AN, Rostami-Hodjegan A, Barber J, and Al-Majdoub ZM (2022) Examining Physiologically Based Pharmacokinetic Model Assumptions for Cross-Tissue Similarity of Activity per Unit of Enzyme: The Case Example of Uridine 5′-Diphosphate Glucuronosyltransferase. *Drug Metab Dispos* **50**:1119–1125.

Basit A, Fan PW, Khojasteh SC, Murray BP, Smith BJ, Heyward S, and Prasad B (2022) Comparison of Tissue Abundance of Non-Cytochrome P450 Drug-Metabolizing Enzymes by Quantitative Proteomics between Humans and Laboratory Animal Species. *Drug Metab Dispos* **50**: 197–203.

Basit A, Neradugomma NK, Wolford C, Fan PW, Murray B, Takahashi RH, Khojasteh SC, Smith BJ, Heyward S, Totah RA, et al. (2020) Characterization of Differential Tissue Abundance of Major Non-CYP Enzymes in Human. *Mol Pharm* **17**:4114–4124.

Bhatt DK, Basit A, Zhang H, Gaedigk A, Lee SB, Claw KG, Mehrotra A, Chaudhry AS, Pearce RE, Gaedigk R, et al. (2018) Hepatic Abundance and Activity of Androgen- and Drug-Metabolizing Enzyme UGT2B17 Are Associated with Genotype, Age, and Sex. *Drug Metab Dispos* **46**: 888–896.

Bhatt DK and Prasad B (2018) Critical Issues and Optimized Practices in Quantification of Protein Abundance Level to Determine Interindividual Variability in DMET Proteins by LC-MS/MS Proteomics. *Clin Pharmacol Ther* **103**:619–630.

Couto N, Al-Majdoub ZM, Gibson S, Davies PJ, Achour B, Harwood MD, Carlson G, Barber J, Rostami-Hodjegan A, and Warhurst G (2020) Quantitative Proteomics of Clinically Relevant Drug-Metabolizing Enzymes and Drug Transporters and Their Intercorrelations in the Human Small Intestine. *Drug Metab Dispos* **48**:245–254.

Drozdzik M, Szelag-Pieniek S, Post M, Zeair S, Wrzesinski M, Kurzawski M, Prieto J, and Oswald S (2020) Protein Abundance of Hepatic Drug Transporters in Patients With Different Forms of Liver Damage. *Clin Pharmacol Ther* **107**:1138–1148.

El-Khateeb E, Al-Majdoub ZM, Rostami-Hodjegan A, Barber J, and Achour B (2021) Proteomic Quantification of Changes in Abundance of Drug-Metabolizing Enzymes and Drug Transporters in Human Liver Cirrhosis: Different Methods, Similar Outcomes. *Drug Metab Dispos* **49**: 610–618.

Fallon JK, Neubert H, Hyland R, Goosen TC, and Smith PC (2013) Targeted quantitative proteomics for the analysis of 14 UGT1As and -2Bs in human liver using NanoUPLC-MS/MS with selected reaction monitoring. *J Proteome Res* **12**:4402–4413.

Fowler S, Kletzl H, Finel M, Manevski N, Schmid P, Tuerck D, Norcross RD, Hoener MC, Spleiss O, and Iglesias VA (2015) A UGT2B10 splicing polymorphism common in african populations may greatly increase drug exposure. *J Pharmacol Exp Ther* **352**: 358–367.

Gasser B, Saloheimo M, Rinas U, Dragosits M, Rodríguez-Carmona E, Baumann K, Giuliani M, Parrilli E, Branduardi P, Lang C, et al. (2008) Protein folding and conformational stress in microbial cells producing recombinant proteins: a host comparative overview. *Microb Cell Fact* **7**:11.

Harbourt DE, Fallon JK, Ito S, Baba T, Ritter JK, Glish GL, and Smith PC (2012) Quantification of human uridine-diphosphate glucuronosyl transferase 1A isoforms in liver, intestine, and kidney using nanobore liquid chromatography-tandem mass spectrometry. *Anal Chem* **84**:98–105.

Harwood MD, Achour B, Neuhoff S, Russell MR, Carlson G, and Warhurst G; Amin Rostami-Hodjegan (2016) In Vitro-In Vivo Extrapolation Scaling Factors for Intestinal P-Glycoprotein and Breast Cancer Resistance Protein: Part I: A Cross-Laboratory Comparison of Transporter-Protein Abundances and Relative Expression Factors in Human Intestine and Caco-2 Cells. *Drug Metab Dispos* **44**:297–307.

Iyer L, Das S, Janisch L, Wen M, Ramírez J, Karrison T, Fleming GF, Vokes EE, Schilsky RL, and Ratain MJ (2002) UGT1A1*28 polymorphism as a determinant of irinotecan disposition and toxicity. *Pharmacogenomics J* **2**:43–47.

Izukawa T, Nakajima M, Fujiwara R, Yamanaka H, Fukami T, Takamiya M, Aoki Y, Ikushiro S, Sakaki T, and Yokoi T (2009) Quantitative analysis of UDP-glucuronosyltransferase (UGT) 1A and UGT2B expression levels in human livers. *Drug Metab Dispos* **37**:1759–1768.

Kamiie J, Ohtsuki S, Iwase R, Ohmine K, Katsukura Y, Yanai K, Sekine Y, Uchida Y, Ito S, and Terasaki T (2008) Quantitative atlas of membrane transporter proteins: development and application of a highly sensitive simultaneous LC/MS/MS method combined with novel in-silico peptide selection criteria. *Pharm Res* **25**:1469–1483.

Kumar AR, Prasad B, Bhatt DK, Mathialagan S, Varma MVS, and Unadkat JD (2020) In Vivo-to-In Vitro Extrapolation of Transporter-Mediated Renal Clearance: Relative Expression Factor Versus Relative Activity Factor Approach. *Drug Metab Dispos* **49**:470–478.

Liao MZ, Gao C, Bhatt DK, Prasad B, and Mao Q (2018) Quantitative Proteomics Reveals Changes in Transporter Protein Abundance in Liver, Kidney and Brain of Mice by Pregnancy. *Drug Metab Lett* **12**:145–152.

Liu JY, Qu K, Sferruzza AD, and Bender RA (2007) Distribution of the UGT1A1*28 polymorphism in Caucasian and Asian populations in the US: a genomic analysis of 138 healthy individuals. *Anticancer Drugs* **18**:693–696.

Margaillan G, Rouleau M, Fallon JK, Caron P, Villeneuve L, Turcotte V, Smith PC, Joy MS, and Guillemette C (2015) Quantitative profiling of human renal UDP-glucuronosyltransferases and glucuronidation activity: a comparison of normal and tumoral kidney tissues. *Drug Metab Dispos* **43**:611–619.

Meech R, Hu DG, McKinnon RA, Mubarokah SN, Haines AZ, Nair PC, Rowland A, and Mackenzie PI (2019) The UDP-Glycosyltransferase (UGT) Superfamily: New Members, New Functions, and Novel Paradigms. *Physiol Rev* **99**:1153–1222.

Parvez MM, Basit A, Jariwala PB, Gáborik Z, Kis E, Heyward S, Redinbo MR, and Prasad B (2021) Quantitative Investigation of Irinotecan Metabolism, Transport, and Gut Microbiome Activation. *Drug Metab Dispos* **49**:683–693.

Prasad B, Achour B, Artursson P, Hop CECA, Lai Y, Smith PC, Barber J, Wisniewski JR, Spellman D, Uchida Y, et al. (2019) Toward a Consensus on Applying Quantitative Liquid Chromatography-Tandem Mass Spectrometry Proteomics in Translational Pharmacology Research: A White Paper. *Clin Pharmacol Ther* **106**:525–543.

Prasad B, Lai Y, Lin Y, and Unadkat JD (2013) Interindividual variability in the hepatic expression of the human breast cancer resistance protein (BCRP/ABCG2): effect of age, sex, and genotype. *J Pharm Sci* **102**:787–793.

Rowland A, Knights KM, Mackenzie PI, and Miners JO (2008) The "albumin effect" and drug glucuronidation: bovine serum albumin and fatty acid-free human serum albumin enhance the glucuronidation of UDP-glucuronosyltransferase (UGT) 1A9 substrates but not UGT1A1 and UGT1A6 activities. *Drug Metab Dispos* **36**:1056–1062.

Sharma S, Suresh Ahire D, and Prasad B (2020) Utility of Quantitative Proteomics for Enhancing the Predictive Ability of Physiologically Based Pharmacokinetic Models Across Disease States. *J Clin Pharmacol* **60** (Suppl 1):S17–S35.

Sipe CJ, Koopmeiners JS, Donny EC, Hatsukami DK, and Murphy SE (2020) *UGT2B10* Genotype Influences Serum Cotinine Levels and Is a Primary Determinant of Higher Cotinine in African American Smokers. *Cancer Epidemiol Biomarkers Prev* **29**:1673–1678.

Vildhede A, Kimoto E, Pelis RM, Rodrigues AD, and Varma MVS (2020) Quantitative Proteomics and Mechanistic Modeling of Transporter-Mediated Disposition in Nonalcoholic Fatty Liver Disease. *Clin Pharmacol Ther* **107**:1128–1137.

Wang L, Collins C, Kelly EJ, Chu X, Ray AS, Salphati L, Xiao G, Lee C, Lai Y, Liao M, et al. (2016) Transporter Expression in Liver Tissue from Subjects with Alcoholic or Hepatitis C Cirrhosis Quantified by Targeted Quantitative Proteomics. *Drug Metab Dispos* **44**:1752–1758.

Wang YH, Trucksis M, McElwee JJ, Wong PH, Maciolek C, Thompson CD, Prueksaritanont T, Garrett GC, Declercq R, Vets E, et al. (2012) UGT2B17 genetic polymorphisms dramatically affect the pharmacokinetics of MK-7246 in healthy subjects in a first-in-human study. *Clin Pharmacol Ther* **92**:96–102.

Wegler C, Gaugaz FZ, Andersson TB, Wiśniewski JR, Busch D, Gröer C, Oswald S, Norén A, Weiss F, Hammer HS, et al. (2017) Variability in Mass Spectrometry-based Quantification of Clinically Relevant Drug Transporters and Drug Metabolizing Enzymes. *Mol Pharm* **14**:3142–3151.

Wenzel C, Drozdzik M, and Oswald S (2021) Mass spectrometry-based targeted proteomics method for the quantification of clinically relevant drug metabolizing enzymes in human specimens. *J Chromatogr B Analyt Technol Biomed Life Sci* **1180**:122891.

Wiśniewski JR (2017) Label-Free and Standard-Free Absolute Quantitative Proteomics Using the "Total Protein" and "Proteomic Ruler" Approaches. *Methods Enzymol* **585**:49–60.

Xue Y, Sun D, Daly A, Yang F, Zhou X, Zhao M, Huang N, Zerjal T, Lee C, Carter NP, et al. (2008) Adaptive evolution of UGT2B17 copy-number variation. *Am J Hum Genet* **83**:337–346.

Address correspondence to: Dr. Bhagwat Prasad, Department of Pharmaceutical Sciences, Washington State University, 412 E Spokane Falls Blvd, Spokane, WA 99202. E-mail: bhagwat.prasad@wsu.edu

Supplementary Information

Quantification of accurate composition and total abundance of homologous proteins by conserved-plus-surrogate peptide (CPSP) approach: Quantification of UDP glucuronosyltransferases in human tissues

Deepak Ahire[1], Mitesh Patel[2], Sujal V. Deshmukh[2], and Bhagwat Prasad[1]
Department of Pharmaceutical Sciences, Washington State University (WSU), Spokane, WA
Novartis Institutes for BioMedical Research, Cambridge, MA

Address Correspondence to:
Bhagwat Prasad, Ph.D.
Department of Pharmaceutical Sciences
Washington State University
Spokane, WA 99202
Telephone: +1-(509) 358-7739
Fax: +1-509-368-6561
E-mail: bhagwat.prasad@wsu.edu

Standardization of UGT1A and UGT2B conserved peptides

The stable isotope-labeled (SIL) UGT1A conserved peptide (IPQTVLWR) was originally procured from Thermo Fisher Scientific (Rockford, IL) without amino acid analysis (AAA). To standardize the SIL form of IPQTVLWR, we used an external calibration method (Bhatt et al., 2019) where the light IPQTVLWR peptide, procured with AAA from New England Peptide (Gardner, MA), was used as a calibrator. UGT2B conserved SIL peptide (VLWR) was standardized by AAA by the vendor (Vivitide, Gardner, MA). The linearity and range of the LC-MS method was verified by measuring the MS responses of the SIL peptides, IPQTVLWR and VLWR from 1.44 to 925.5 and 0.33 to 170.5 fmol/µL, respectively.

Supplementary Table 1: List of conserved and surrogate peptides used for targeted LC-MS/MS quantification of UGT proteins. Light peptides are unlabeled, whereas heavy peptides contain stably labeled (^{13}C and ^{15}N) R or K

Protein	Peptide sequence	Peptide label	Parent ion (m/z)	Product ion (m/z)	CE (eV)	Cone voltage (V)
Conserved peptides						
UGT1A	IPQTVLWR	Light	506.8	802.4	16	35
	IPQTVLWR	Light	506.8	674.4	16	35
	IPQTVLWR	Light	506.8	573.3	16	35
	IPQTVLWR	Heavy	511.8	812.4	16	35
	IPQTVLWR	Heavy	511.8	684.4	16	35
	IPQTVLWR	Heavy	511.8	583.4	16	35
UGT2B	VLWR	Light	287.2 (+2)	474.2	10	35
	VLWR	Light	287.2 (+2)	361.2	10	35
	VLWR	Light	287.2 (+2)	213.2	10	35
	VLWR	Heavy	292.1 (+2)	484.3	10	35
	VLWR	Heavy	292.1 (+2)	371.2	10	35
	VLWR	Heavy	292.1 (+2)	213.2	10	35
Surrogate peptides						
UGT1A1	DGAFYTLK	Light	457.7 (+2)	671.4	16	35
	DGAFYTLK	Light	457.7 (+2)	260.2	16	35
	DGAFYTLK	Light	457.7 (+2)	244.1	16	35
	DGAFYTLK	Heavy	461.7 (+2)	679.4	16	35
	DGAFYTLK	Heavy	461.7 (+2)	268.2	16	35
	DGAFYTLK	Heavy	461.7 (+2)	244.1	16	35
	ESFVSLGHNVFENDSFLQR	Light	742.4 (+3)	650.4	25	35
	ESFVSLGHNVFENDSFLQR	Light	742.4 (+3)	303.2	25	35
	ESFVSLGHNVFENDSFLQR	Light	742.4 (+3)	881.9	25	35
	ESFVSLGHNVFENDSFLQR	Heavy	745.7 (+3)	660.4	25	35
	ESFVSLGHNVFENDSFLQR	Heavy	745.7 (+3)	313.2	25	35
	ESFVSLGHNVFENDSFLQR	Heavy	745.7 (+3)	886.9	25	35
UGT1A3	YLSIPTVFFLR	Light	678.4 (+2)	1079.6	24	35
	YLSIPTVFFLR	Light	678.4 (+2)	879.5	24	35
	YLSIPTVFFLR	Light	678.4 (+2)	277.2	24	35
	YLSIPTVFFLR	Heavy	683.4 (+2)	1089.6	24	35
	YLSIPTVFFLR	Heavy	683.4 (+2)	889.5	24	35

	YLSIPTVFFLR	Heavy	683.4 (+2)	277.2	24	35
UGT1A4	VTLGYTQGFFETEHLLK	Light	661.7 (+2)	1016.5	22	35
	VTLGYTQGFFETEHLLK	Light	661.7 (+2)	892	22	35
	VTLGYTQGFFETEHLLK	Light	661.7 (+2)	835.4	22	35
	VTLGYTQGFFETEHLLK	Heavy	664.4 (+2)	1024.6	22	35
	VTLGYTQGFFETEHLLK	Heavy	664.4 (+2)	896	22	35
	VTLGYTQGFFETEHLLK	Heavy	664.4 (+2)	839.4	22	35
	GTQCPNPSSYIPK	Light	724.8 (+2)	791.4	30	35
	GTQCPNPSSYIPK	Light	724.8 (+2)	581.7	30	35
	GTQCPNPSSYIPK	Heavy	728.8 (+2)	799.4	30	35
	GTQCPNPSSYIPK	Heavy	840.9 (+2)	585.7	30	35
UGT1A6	SFLTAPQTEYR	Light	656.8 (+2)	965.5	23	35
	SFLTAPQTEYR	Light	656.8 (+2)	864.4	23	35
	SFLTAPQTEYR	Light	656.8 (+2)	793.4	23	35
	SFLTAPQTEYR	Heavy	661.8 (+2)	975.5	23	35
	SFLTAPQTEYR	Heavy	661.8 (+2)	874.4	23	35
	SFLTAPQTEYR	Heavy	661.8 (+2)	803.4	23	35
	DIVEVLSDR	Light	523.3 (+2)	718.4	18	35
	DIVEVLSDR	Light	523.3 (+2)	589.3	18	35
	DIVEVLSDR	Heavy	528.3 (+2)	728.4	18	35
	DIVEVLSDR	Heavy	528.3 (+2)	599.3	18	35
UGT1A7 & UGT1A8	YFSLPSVVFAR	Light	643.3 (+2)	775.4	23	35
	YFSLPSVVFAR	Light	643.3 (+2)	388.2	23	35
	YFSLPSVVFAR	Light	643.3 (+2)	311.1	23	35
	YFSLPSVVFAR	Heavy	648.3 (+2)	785.4	23	35
	YFSLPSVVFAR	Heavy	648.3 (+2)	393.2	23	35
	YFSLPSVVFAR	Heavy	648.3 (+2)	311.1	23	35
UGT1A7	TYSTSYTLEDQD	Light	789.8 (+2)	662.2	23	35
	TYSTSYTLEDQD	Light	789.8 (+2)	775.3	23	35
	TYSTSYTLEDQD	Light	789.8 (+2)	876.4	23	35
	TYSTSYTLEDQD	Heavy	794.8 (+2)	672.2	23	35
	TYSTSYTLEDQD	Heavy	794.8 (+2)	785.3	23	35
	TYSTSYTLEDQD	Heavy	794.8 (+2)	886.4	23	35
UGT1A8	GIACHYLEEGAQCPAPLSYVP	Light	830.0 (+3)	831.4	23	45
	GIACHYLEEGAQCPAPLSYVP	Light	830.0 (+3)	601.2	23	45
	GIACHYLEEGAQCPAPLSYVP	Light	830.0 (+3)	665.3	23	45
	GIACHYLEEGAQCPAPLSYVP	Heavy	833.4 (+3)	65.3	23	45
	GIACHYLEEGAQCPAPLSYVP	Heavy	833.4 (+3)	601.2	23	45
	GIACHYLEEGAQCPAPLSYVP	Heavy	833.4 (+3)	841.4	23	45

UGT1A9	AFAHAQWK	Light	320.2	444.2	23	35
	AFAHAQWK	Light	320.2	370.7	23	35
	AFAHAQWK	Light	320.2	335.2	23	35
	AFAHAQWK	Heavy	322.8	448.2	23	35
	AFAHAQWK	Heavy	322.8	374.7	23	35
	AFAHAQWK	Heavy	322.8	339.2	23	35
UGT1A10	YFSLPSVVFTR	Light	658.4 (+2)	1005.6	23	35
	YFSLPSVVFTR	Light	658.4 (+2)	805.5	23	35
	YFSLPSVVFTR	Light	658.4 (+2)	398.2	23	35
	YFSLPSVVFTR	Heavy	663.4 (+2)	1015.6	23	35
	YFSLPSVVFTR	Heavy	663.4 (+2)	815.5	23	35
	YFSLPSVVFTR	Heavy	663.4 (+2)	398.2	23	35
UGT2B4	FEVYPVSLTK	Light	591.8 (+2)	906.5	21	35
	FEVYPVSLTK	Light	591.8 (+2)	807.5	21	35
	FEVYPVSLTK	Light	591.8 (+2)	644.4	21	35
	FEVYPVSLTK	Heavy	595.8 (+2)	914.5	21	35
	FEVYPVSLTK	Heavy	595.8 (+2)	815.5	21	35
	FEVYPVSLTK	Heavy	595.8 (+2)	652.4	21	35
	TILDELVQR	Light	543.8 (+2)	872.5	19	35
	TILDELVQR	Light	543.8 (+2)	759.4	19	35
	TILDELVQR	Light	543.8 (+2)	644.4	19	35
	TILDELVQR	Heavy	548.8 (+2)	882.5	19	35
	TILDELVQR	Heavy	548.8 (+2)	769.4	19	35
	TILDELVQR	Heavy	548.8 (+2)	654.4	19	35
UGT2B7	ANVIASALAQIPQK	Light	712.4 (+2)	797.5	25	35
	ANVIASALAQIPQK	Light	712.4 (+2)	684.4	25	35
	ANVIASALAQIPQK	Light	712.4 (+2)	372.2	25	35
	ANVIASALAQIPQK	Heavy	716.4 (+2)	805.5	25	35
	ANVIASALAQIPQK	Heavy	716.4 (+2)	692.4	25	35
	ANVIASALAQIPQK	Heavy	716.4 (+2)	380.2	25	35
	IEIYPTSLTK	Light	582.8 (+2)	922.5	20	35
	IEIYPTSLTK	Light	582.8 (+2)	646.4	20	35
	IEIYPTSLTK	Heavy	586.8 (+2)	930.5	20	35
	IEIYPTSLTK	Heavy	586.8 (+2)	654.4	20	35
	TILDELIQR	Light	550.8 (+2)	886.5	19	35
	TILDELIQR	Light	550.8 (+2)	658.4	19	35
	TILDELIQR	Light	550.8 (+2)	416.3	19	35
	TILDELIQR	Heavy	555.8 (+2)	896.5	19	35
	TILDELIQR	Heavy	555.8 (+2)	668.4	19	35

	TILDELIQR	Heavy	555.8 (+2)	426.3	19	35
UGT2B10	TEFENIIMQLVK	Light	732.9 (+2)	731.4	25	35
	TEFENIIMQLVK	Light	732.9 (+2)	618.3	25	35
	TEFENIIMQLVK	Light	732.9 (+2)	487.3	25	35
	TEFENIIMQLVK	Heavy	736.9 (+2)	739.4	25	35
	TEFENIIMQLVK	Heavy	736.9 (+2)	626.3	25	35
	TEFENIIMQLVK	Heavy	736.9 (+2)	495.3	25	35
UGT2B15	SVINDPVYK	Light	517.8 (+2)	848.5	18	35
	SVINDPVYK	Light	517.8 (+2)	735.4	18	35
	SVINDPVYK	Light	517.8 (+2)	424.7	18	35
	SVINDPVYK	Heavy	521.8 (+2)	856.5	18	35
	SVINDPVYK	Heavy	521.8 (+2)	743.4	18	35
	SVINDPVYK	Heavy	521.8 (+2)	428.7	18	35
	NYLEDSLLK	Light	547.8 (+2)	817.5	19	35
	NYLEDSLLK	Light	547.8 (+2)	704.4	19	35
	NYLEDSLLK	Light	547.8 (+2)	278.1	19	35
	NYLEDSLLK	Heavy	551.8 (+2)	825.5	19	35
	NYLEDSLLK	Heavy	551.8 (+2)	712.4	19	35
	NYLEDSLLK	Heavy	551.8 (+2)	278.1	19	35
UGT2B17	FSVGYTVEK	Light	515.3 (+2)	882.5	18	35
	FSVGYTVEK	Light	515.3 (+2)	795.4	18	35
	FSVGYTVEK	Light	515.3 (+2)	696.4	18	35
	FSVGYTVEK	Heavy	519.3 (+2)	890.5	18	35
	FSVGYTVEK	Heavy	519.3 (+2)	803.4	18	35
	FSVGYTVEK	Heavy	519.3 (+2)	704.4	18	35
	SVINDPIYK	Light	524.8 (+2)	862.5	18	35
	SVINDPIYK	Light	524.8 (+2)	749.4	18	35
	SVINDPIYK	Light	524.8 (+2)	431.7	18	35
	SVINDPIYK	Heavy	528.8 (+2)	870.5	18	35
	SVINDPIYK	Heavy	528.8 (+2)	757.4	18	35
	SVINDPIYK	Heavy	528.8 (+2)	435.7	18	35

Supplementary Table 2: Chromatographic conditions to separate UGT surrogate and conserved peptides			
Guard column: Acquity HSS T3 column (100Å, 1.8 µm, 2.1mm * 5 mm			
Acquity UPLC HSS T3 column (100Å, 1.8 µm, 1 mm * 100 mm)			
Injection volume: 1 µL			
LC gradient program			
Time (min)	Flow Rate (µL)	A (Water with 0.1% formic acid, %)	B (Acetonitrile with 0.1% formic acid, %)
0	50	97	3
4	50	97	3
8	50	87	13
18	50	70	30
20.5	50	65	35
21.1	50	40	60
23.1	50	20	80
23.2	50	97	3
27	50	97	3

Supplementary Table 3: UGTs abundance (pmol/mg microsomal protein) in HLM, HIM, HKM, and HLS9				
UGT isoform	HLM	HIM	HKM	HLS9
UGT1A1	85.01 ± 4.42	9.65 ± 1.37	<LLOQ	14.14 ± 1.88
UGT1A3	12.57 ± 2.37	0.93 ± 0.04	<LLOQ	2.76 ± 0.08
UGT1A4	88.26 ± 8.63	<LLOQ	<LLOQ	10.73 ± 0.64
UGT1A6	26.92 ± 1.87	<LLOQ	47.98 ± 7.00	3.01 ± 0.38
UGT1A7	<LLOQ	<LLOQ	<LLOQ	<LLOQ
UGT1A8	<LLOQ	<LLOQ	<LLOQ	<LLOQ
UGT1A9	31.14 ± 2.45	<LLOQ	69.69 ± 12.16	5.95 ± 0.43
UGT1A10	<LLOQ	6.26 ± 0.1	<LLOQ	<LLOQ
UGT2B4	71.09 ± 3.48	<LLOQ	<LLOQ	11.49 ± 0.40
UGT2B7	112.83 ± 6.08	16.54 ± 6.39	59.77 ± 2.10	20.92 ± 1.07
UGT2B10	76.46 ± 16.04	<LLOQ	<LLOQ	10.92 ± 0.20
UGT2B15	75.05 ± 5.13	<LLOQ	<LLOQ	9.76 ± 0.28
UGT2B17	16.80 ± 4.97	52.23 ± 6.02	<LLOQ	2.59 ± 0.17
LLOQ: lower limit of quantification				

Supplemental Figures

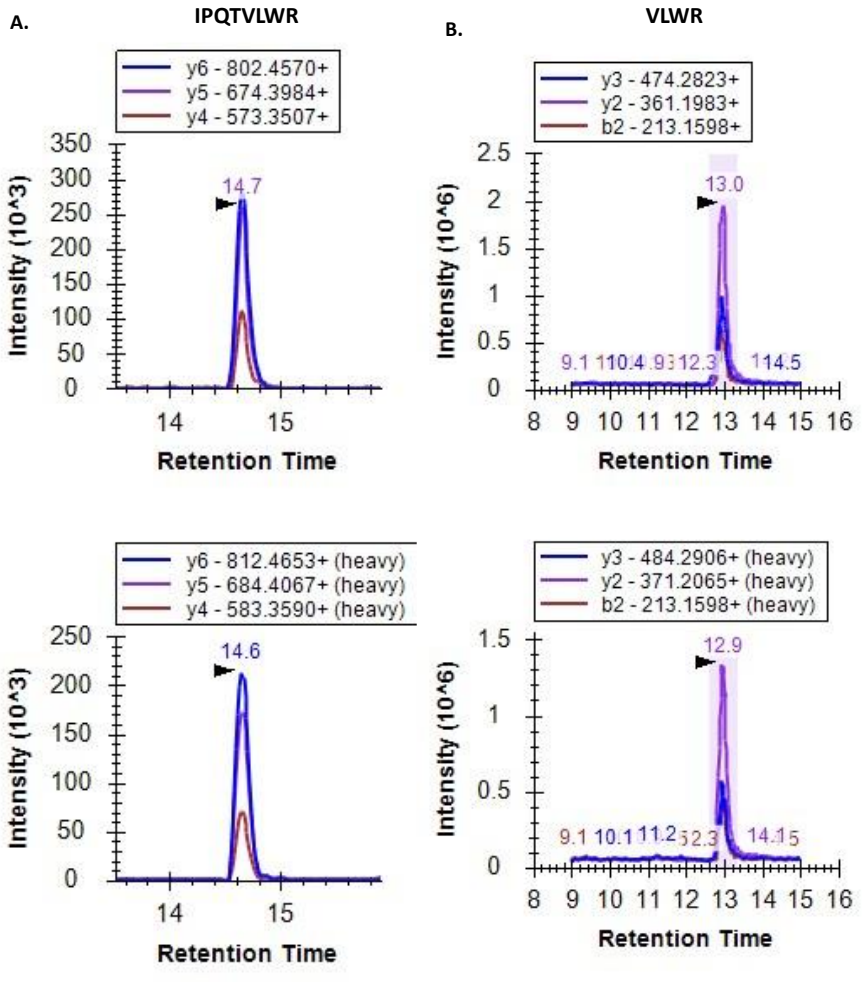

Supplementary Fig. 1. Representative chromatogram of two conserved peptides, IPQTVLWR (A) and VLWR (B) used in the quantification of UGT1A and UGT2B enzymes, respectively.

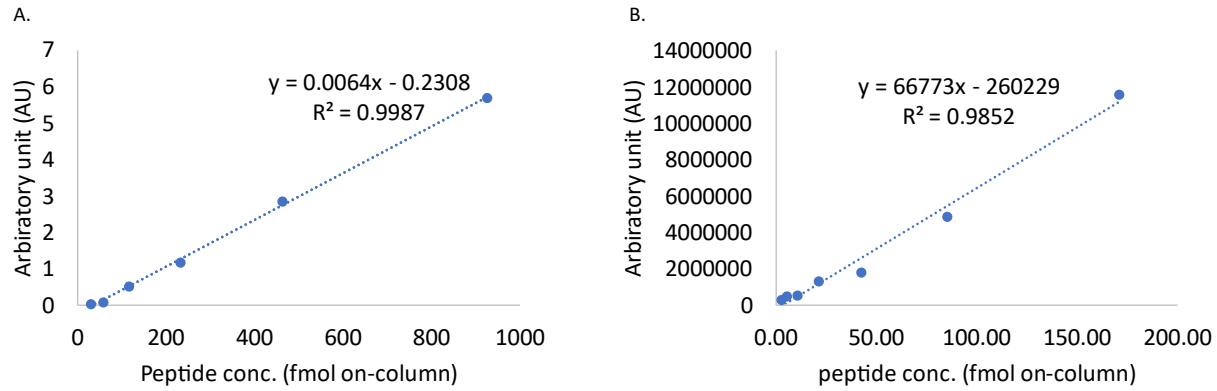

Supplementary Fig. 2. The calibration curves of the conserved peptides, IPQTVLWR (A) and VLWR, (B) were linear between 58 to 925 and 0.33 to 170.75 fmol on-column, respectively with R^2 >0.98.

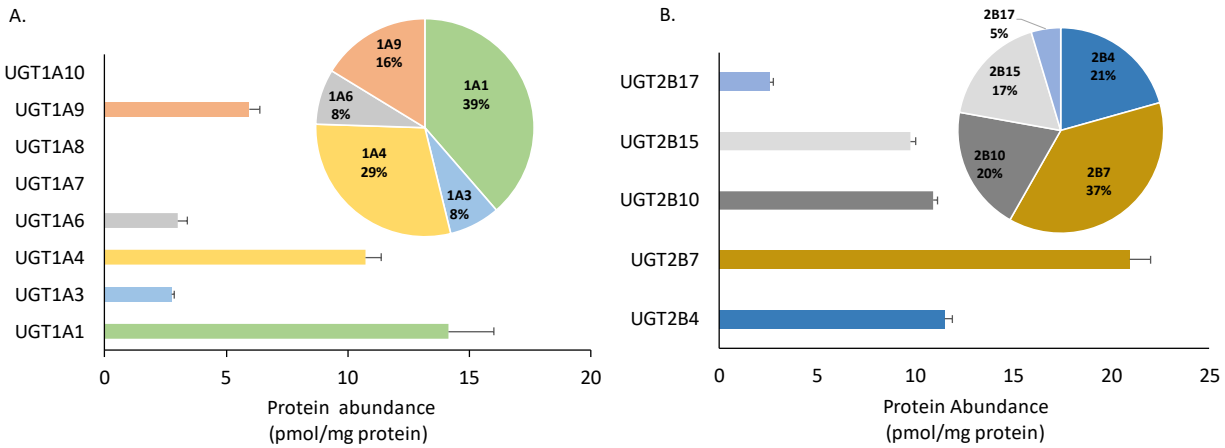

Supplementary Fig. 3. The abundance of UGT1As (A) and UGT2Bs (B) using the conserved peptide approach in the HLS9 fractions.

Reference

Bhatt DK, Mehrotra A, Gaedigk A, Chapa R, Basit A, Zhang H, Choudhari P, Boberg M, Pearce RE, Gaedigk R, Broeckel U, Leeder JS, and Prasad B (2019) Age- and Genotype-Dependent Variability in the Protein Abundance and Activity of Six Major Uridine Diphosphate-Glucuronosyltransferases in Human Liver. *Clin Pharmacol Ther* **105:**131-141.